Received: 26 June 2023 | Revised: 20 November 2023 | Accepted: 27 November 2023

DOI: 10.1002/hyp.15045

RESEARCH ARTICLE

WILEY

Complex canopy structures control tree transpiration: A study based on 3D modelling in a tropical rainforest

Alexander Röll[1,2] | Tongming Kang[1] | Peter Hahn[1] | Joyson Ahongshangbam[1,3] | Florian Ellsäßer[1,4] | Hendrayanto[5] | Puja Sharma[1,6] | Thorge Wintz[1] | Dirk Hölscher[1,7]

[1]Tropical Silviculture and Forest Ecology, University of Göttingen, Göttingen, Germany

[2]Horticultural Sciences, Institute for Crop Science and Resource Conservation, University of Bonn, Bonn, Germany

[3]Institute for Atmospheric and Earth System Research, University of Helsinki, Helsinki, Finland

[4]Department for Natural Resources, University of Twente, ITC, Enschede, the Netherlands

[5]Forest Management Department, Bogor Agricultural University, Bogor, Indonesia

[6]Department of Biological Sciences, University of Notre Dame, Notre Dame, Indiana, USA

[7]Centre of Biodiversity and Sustainable Land Use, University of Göttingen, Göttingen, Germany

Correspondence
Alexander Röll, Tropical Silviculture and Forest Ecology, University of Göttingen, Büsgenweg 1, Göttingen 37077, Germany.
Email: aroell@gwdg.de

Funding information
Deutsche Forschungsgemeinschaft

Abstract

Tropical rainforests are rich in tree species and comprise complex canopy structures. Transpiration by forest trees is a major hydrological flux which contributes to climate regulation. We explored the role of forest canopy structure on tree transpiration in a tropical rainforest on Sumatra, Indonesia. Drone-based photogrammetry and the structure from motion technique were used to compute high-resolution 3D point clouds and derive forest and tree structural variables. Transpiration of differently sized and vertically positioned trees was assessed with sap flux measurements. Per-tree transpiration rates increased linearly with several variables related to crown dimension and were further enhanced by top-heavy crown shape, dense leafage and increasing canopy openness as assessed with the gap light index. Under given environmental conditions, the two variables crown volume and top-heaviness explained 74% of the observed variance in per-tree transpiration. Transpiration rates per unit crown dimension were highest for small crowns, decreased non-linearly with increasing crown dimension and were little affected by other analysed structural variables. Our study underlines the potential of 3D point cloud analyses for accurately determining the structure of complex forest canopies and thus better understanding and predicting transpiration rates of differently positioned trees.

KEYWORDS
crown metrics, drone, gap light index, Indonesia, leaf area index, photogrammetry, point cloud, sap flux, Sumatra, UAV

1 | INTRODUCTION

Tropical rainforests provide key ecosystem services such as (evapo)transpiration, which contributes to atmospheric cooling, cloud formation and turbulence (Ellison et al., 2017; Fisher et al., 2009). Trees are the main agents of transpiration in tropical rainforests. The individual rainforest trees are highly variable regarding crown dimension, architecture, leaf density and canopy position, which likely influences their transpiration rates. Due to the overall high structural complexity and diversity, studying the spatial controls of transpiration in tropical rainforests is challenging.

In general, per-tree transpiration often scales with tree size. Variations among trees are thus often explained by biometric variables,

among which stem diameter is often applied (Dierick & Hölscher, 2009; Kotowska et al., 2021; Meinzer et al., 2001; Vertessy et al., 1995; Wang et al., 2019; Yue et al., 2008). However, crown dimension-related metrics such as crown projection area were reported to perform better than stem diameter for predicting transpiration, for example, across 32 study sites in lowland Sumatra (Röll et al., 2019). Aerial close-surface photography with drones provides new ways to assess canopy structures (Wallace et al., 2016). With the structure from motion technique (SfM, Lowe, 2004), Red-Green-Blue (RGB) images acquired with an Uncrewed Aerial Vehicle (UAV) can be used to construct high-density point clouds, which allow for a detailed analysis of the canopy (Dietmaier et al., 2019; Iglhaut et al., 2019; Khokthong et al., 2019). Previous studies from drones over a tropical agroforest and a tropical rainforest showed that crown dimension variables derived from 3D point clouds explained substantially more of the variance in per-tree transpiration than the classic variable stem diameter (Ahongshangbam et al., 2019, 2020). However, a considerable amount of unexplained variability remained.

Variations in per-tree transpiration that are not explained by crown dimension alone may be related to differences in crown shape, crown leaf density or crown exposure. Considering potential interactive effects of such canopy variables with crown dimension-related variables may further improve our understanding of tropical rainforest transpiration. Trees show high plasticity in crown shapes in response to exposure to light and other factors (Harja et al., 2012), which likely affects their transpiration. However, studies investigating effects of crown shape on transpiration are rare. We found only one previous study, which reported higher per-tree transpiration when crown heterogeneity was maximized within a given space compared to more uniformly shaped crowns (Bauerle et al., 2004).

For estimating the crown leaf density-related variables leaf area index (LAI) or leaf area density (LAD), several previous studies applied point cloud methods, typically derived from light detection and ranging (LiDAR) methods (e.g., de Almeida et al., 2019; Richardson et al., 2009; Zhao & Popescu, 2009). More recently, photogrammetrically-derived point clouds based on aerial imagery were reported to also produce reliable LAI estimates (Comba et al., 2020). LAI is often incorporated into water flux models at the stand-scale, wherein up to a certain threshold higher LAI leads to higher (evapo)transpiration (e.g., Birhanu et al., 2019; Farid et al., 2008; Wang et al., 2014). The total leaf area per tree, which can be estimated as the product of LAI and crown projection area (or the product of LAD and crown volume), was found to be positively correlated with per-tree transpiration in several previous studies (Palmer et al., 2009; Radersma et al., 2006; Sala et al., 1996; Vertessy et al., 1997). However, to our knowledge such assessments have not yet been carried out in complex tropical forest canopies.

Tree transpiration is further controlled by environmental factors such as light availability (Jarvis, 1976). Temporal variations in transpiration are commonly explained well by micrometeorological fluctuations, given that soil moisture remains above critical thresholds (Dierick & Hölscher, 2009; Hardanto et al., 2017; McJannet et al., 2007; Röll et al., 2019; Wallace & McJannet, 2010). Small-scale spatial variations in environmental factors as for example, induced by canopy gaps have only rarely been connected to tree transpiration (e.g., Zhang et al., 2019). One might expect that per-tree transpiration increases with increasing crown exposure, that is, increasing light availability. However, for some shade tolerant understory species, previous studies reported decreasing per-tree transpiration with increasing canopy openness (Köhler et al., 2009; van Kanten & Vaast, 2006). For assessing light availability at different canopy positions, hemispherical photographs can be used (Roxburgh & Kelly, 1995). A method of generating synthetic (virtual) hemispherical photographs (SHPs) from 3D point clouds was established by Moeser et al. (2014); the SHPs produced accurate estimates of canopy closure and LAI compared to actual hemispherical photographs. SHPs taken at the top of a given tree within a point cloud can be used to estimate light availability (Cifuentes et al., 2017; Van der Zande et al., 2011), for example, via the gap light index (GLI, Canham, 1988). A recent study concluded that SHPs generated from photogrammetry-based point clouds work very well for estimating light transmission (Brüllhardt et al., 2020).

In addition to studies on per-tree transpiration, transpiration rates of (rainforest) trees per unit crown dimension are of particular ecohydrological interest (Wullschleger et al., 1998). Therein, a commonly studied variable is the transpiration per unit ground projection area, commonly expressed in mm time^{-1}. However, many (tropical) transpiration studies focus on stand transpiration rates rather than tree-level analysis (e.g., Aparecido et al., 2016; Kunert et al., 2015; McJannet et al., 2007; Röll et al., 2019). In previous tree-level studies including one in a tropical rainforest, up to 15-fold differences in transpiration per unit ground area were reported among trees of different species and of different sizes (Dawson, 1996; Ewers et al., 2002; Jordan & Kline, 1977). Similarly, previous studies assessing transpiration per unit leaf area reported substantial differences among tree species as well as intra-specific differences among provenances, fertilization levels, tree ages and sites (Deans & Munro, 2004; Hubbard et al., 1999; Radersma et al., 2006; Santiago et al., 2000). To our knowledge, transpiration rates per unit crown dimension have only rarely been assessed comprehensively for tropical rainforest trees (e.g., Kunert et al., 2017).

In our study, we used point clouds derived from drone-based photogrammetry for canopy and tree crown analyses and performed sap flux measurements for estimating per-tree transpiration of 42 rainforest trees in lowland Sumatra, Indonesia. The objective of our study was to assess the spatial, tree-level controls of transpiration, with emphasis on variables of crown dimension, shape, leaf density and light exposure.

2 | MATERIALS AND METHODS

2.1 | Study region and sites

The study was conducted in the Harapan rainforest in Jambi province, Sumatra, Indonesia, on five 50 m × 50 m plots (plot codes: HF2,

HFr1, HFr2, HFr3, HFr4; Figure 1) which are core plots of the EFForTS project (Drescher et al., 2016). The average annual temperature is 26.7°C and mean annual precipitation is 2390 mm. There is no pronounced dry season, with all months typically receiving more than 100 mm of precipitation (Drescher et al., 2016). The terrain is undulating, dividing the forest into upland and riparian sites (Ahongshangbam et al., 2020). The forest is rich in tree species (Rembold et al., 2017) but has a history of logging (Harrison & Swinfield, 2015).

2.2 | Tree transpiration

To derive tree transpiration rates, sap flux measurements were successively conducted across the five plots between August and December 2016. Twelve trees were studied in plot HF2 and 15 trees each in the other plots, adding up to a total of 72 sap flux trees. The crowns of all sap flux trees had access to the upper canopy layers and where thus (mostly) visible from above (Figure 2, Figure S1); therein, the trees relatively evenly encompassed smaller to larger diameters at breast height (DBH, min. 14 cm, max. 57 cm), tree height (min. 14 m, max. 41 m) and crown dimension (min. 36 m^3 crown volume; max. 1604 m^3) (Tables S1 and S2). On these trees, we measured sap flux density (J_S, g cm^{-2} h^{-1}) with thermal dissipation probes (Granier, 1985). The original Granier equation parameters were reported to yield good estimates of J_S for forests in the same region (Röll et al., 2019) and were therefore applied in the present study. To estimate water conductive areas (cm^2) for each tree, we used a relationship between DBH and water conductive area as presented for forest trees in lowland Sumatra based on radial J_S measurements with heat field deformation sensors (Röll et al., 2019). Per-tree transpiration rates (kg day^{-1}) were calculated by multiplying daily accumulated sap flux by the respective water conductive areas. For each sample tree, several days to several weeks of transpiration data were available, from which the day with the highest transpiration rate was selected for this study, thus focusing on maximum observed per-tree transpiration. Transpiration rates per unit crown dimension were calculated by dividing daily per-tree transpiration by crown volume, surface area, projection area or total leaf area, respectively; additionally, the transpiration per unit leaf area density was calculated (see Table S1).

2.3 | Point cloud analysis

2.3.1 | Drone imaging and tree identification

Point clouds of the study plots were acquired based on drone-recorded RGB imagery and the structure from motion (SfM) technique (Lowe, 2004). One drone flight was conducted per study plot, always in parallel to the sap flux measurements, using a multirotor UAV (MikroKopter EASY Okto V3, HiSystems) equipped with an RGB camera (Sony Alpha 5000 with Sony E PZ lens fixed to 16 mm). The drone travelled along a circular route in a superposing manner at a flight altitude between 63 and 82 m above ground (Table 1). Drone GPS data logged along with the images was used for georeferencing, blurry images and images of low quality were removed. The images were aligned and dense point clouds were created using Agisoft Photoscan Professional 1.2.6 (Agisoft LLC, 2019) with standard settings, that is, without automatic gap filling or further corrections. Based on the point cloud data, 2D orthomosaics of the study plots and their

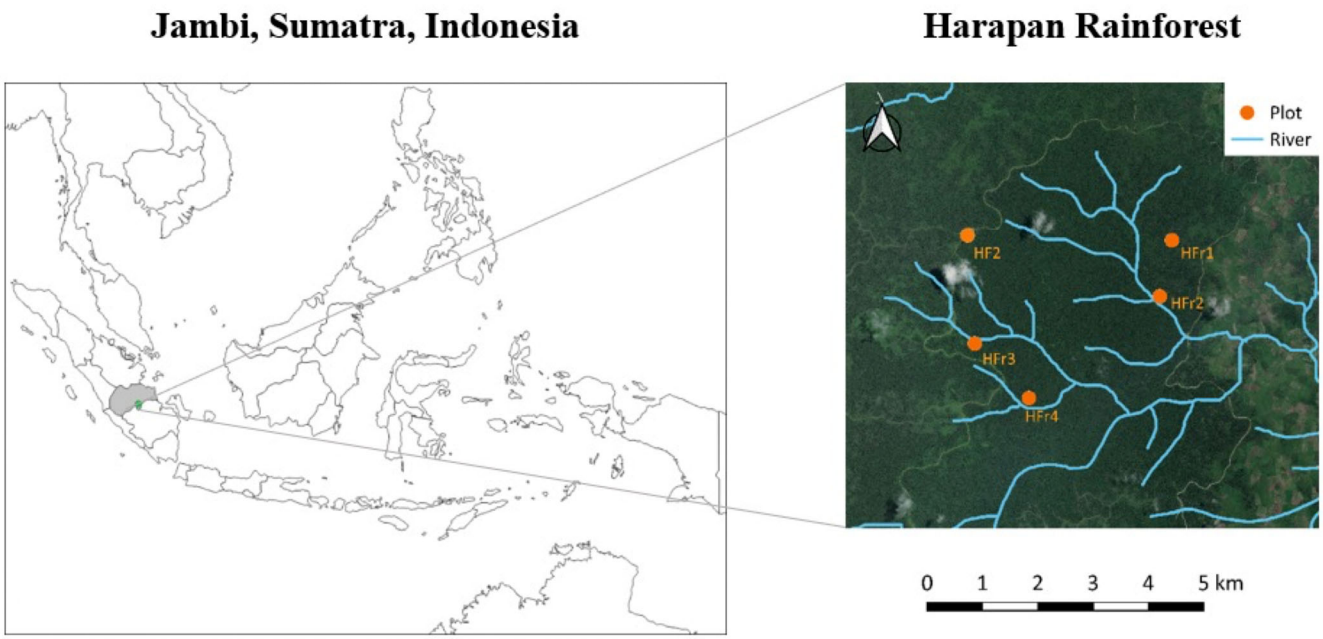

FIGURE 1 Overview of the lowland study region and the five study plots (HF2, HFr1, HFr2, HFr3, HFr4) in the Harapan rainforest, Jambi province, Sumatra, Indonesia. The plots are 50 m × 50 m in size.

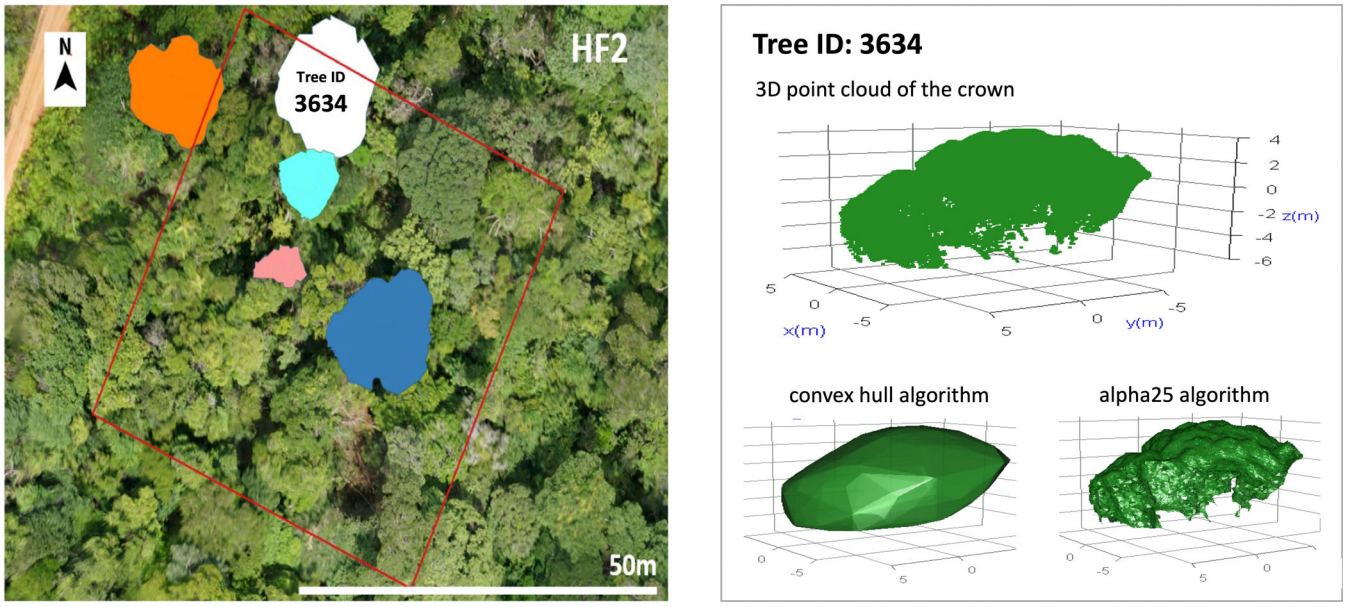

FIGURE 2 Example of the 3D point cloud workflow for one sample tree (ID 3634) in one study plot (HF2). In the processed RGB orthomosaic (left panel), the plot boundaries are delineated (red line) and a given sap flux sample tree is located manually based on data from ground assessments. The crown of each clearly identified sap flux sample tree is then delineated manually (differently coloured shapes). The according crowns (right panel) are extracted from the plot 3D point clouds, are refined manually and are subsequently subjected to different algorithms (e.g., convex hull, alpha25) as the basis for calculating diverse crown metrics (see overview in Table S1). The plot orthomosaics of all study plots can be found in Figure S1, the crowns of all sample trees in Figure S2.

surroundings were created (Figure 2, Figure S1). On average 195 RGB images per plot were used to create the point clouds with densities from 610 to 990 points m^{-2} and a ground resolution of 1.62 to 2.07 cm $pixel^{-1}$ (Table 1).

The stem base locations of the sap flux trees and neighbouring trees within all plots were recorded on a tree location map with Cartesian coordinates during the field work. The GPS coordinates of the plot corners were recorded and used to georeference the tree location maps in UTM WGS 84 using QGIS 3.10 (QGIS, 2020, http://www.qgis.org/). The georeferenced tree location maps were superimposed over the RGB orthomosaics to identify the sap flux trees. Information on stem position and basic characteristics (stem diameters, tree heights) as available from a ground inventory along with a close visual examination of RGB orthomosaics, canopy height models and 3D point clouds were used for the tree identification. However, identifying the sap flux trees was challenging due to the high density of tree crowns and multi-layered structure of the canopy. In total, 42 out of 72 sap flux trees were clearly identified in the aerial images and thus used as the sample in our study (Figure S1, Table S2). For each of the 42 identified trees, the crowns were subsequently manually delineated in the 2D orthomosaics as a polygon using QGIS. The corresponding 3D point clouds within each polygon were then clipped using the *lasclip* function of the *lidR* R package (Roussel & Auty, 2018). The individual crown point clouds were manually segmented from neighbouring crowns and refined using the software Cloud Compare v.2.9 (CloudCompare, 2019), including the removal of outliers, as the basis for calculating canopy metrics (Figure 2, Figure S2).

2.3.2 | Crown dimension metrics

For the calculation of different crown dimension variables, we used the *rLIDAR* R package (Silva et al., 2015). As a baseline variable we used the crown volume (m^3) as derived from a convex hull algorithm (in the following referred to as 'crown volume'), which was reported to be a good predictor of per-tree transpiration in previous studies in the same region and partly on the same sample trees (Ahongshangbam et al., 2019, 2020; note: crown volume of one tree was corrected from the dataset of Ahongshangbam et al., 2020). As additional crown dimension variables, we calculated crown width (m, average of a North–South and an East–West measurement), the ground projection area (m^2) of the convex hull crown body into the 2D plane (in the following referred to as 'ground projection area', in other studies also called 'crown projection area'; note: ground projection area of several trees were corrected from the dataset of Ahongshangbam et al., 2020), the crown surface area (m^2) as derived from an alpha25-algorithm (in the following referred to as 'crown surface area'; note: these values differ from the convex hull surface areas as presented in Ahongshangbam et al., 2020) and the crown volume of the upper crown half (m^3, convex hull) (Table S1). The total leaf area per tree, which was calculated by multiplying the ground projection area by the leaf-related variable leaf area index (see description in Section 2.3.4), is listed as a variable of crown dimension in our study due to its close correlation with other dimension-related metrics ($R \geq 0.77$, Figures S3 and S4).

TABLE 1 Characteristics of the drone missions and the derived point clouds.

Plot	Flight altitude (m)	Aligned aerial photos (images plot^{-1})	Point density (points m^{-2})	Ground resolution (cm pixel^{-1})
HF2	75	181	941	1.83
HFr1	80	214	708	1.95
HFr2	82	207	610	2.07
HFr3	67	203	929	1.69
HFr4	63	170	990	1.62

2.3.3 | Crown shape-related variables

At any given dimension (see Section 2.3.2), similar-sized crowns may still differ vastly in appearance and functioning due to differences in crown shape. From the refined crown point clouds, the height of each crown was calculated by subtracting the minimum observed z-value within each crown from the respective maximum z-value (the z-value characterizes the elevation of a given voxel within a 3D point cloud, see Figure 2). Then, the crown width-to-height ratio as an indicator of crown shape was calculated by dividing crown height by the formerly derived crown width. Crown top-heaviness was calculated as the ratio of crown volume of the upper crown half to total crown volume. Crown roughness length (m^2 m^{-2}) was calculated as the crown surface area divided by the ground projection area. An overview of the crown shape-related variables and their calculation can be found in Table S1.

2.3.4 | Crown leaf density-related variables

The 42 individual crown point clouds were used as input for the *leafR* R package (de Almeida et al., 2019) to derive estimates of leaf area index (LAI, m^2 m^{-2}) for each sample tree. We further calculated leaf area density (LAD, m^2 m^{-3}) by dividing the total leaf area per tree by crown volume (see description in Section 2.3.1). An overview of the leaf density-related variables and their calculation can be found in Table S1.

2.3.5 | Exposure-related variables

The gap light index (GLI, Canham, 1988) is an indicator of understory light levels in forests based on a very strong correlation observed between light transmission expressed in percentage and GLI ($r = 0.93$) (Canham, 1988). GLI ranges from 0, when there is no clearly visible gap in the canopy, to 1 for a completely open area without any crown cover (Hu & Zhu, 2008) and is calculated as follows:

$$\mathrm{GLI} = T_{\mathrm{diffuse}} P_{\mathrm{diffuse}} + T_{\mathrm{beam}} P_{\mathrm{beam}},$$

where P_{diffuse} and P_{beam} are the proportions of incoming photosynthetically active radiation received at the top of the canopy in the form of diffuse sky radiation and direct beam radiation respectively, and T_{diffuse} and T_{beam} are the proportions of diffuse and beam radiation that are transmitted through the canopy to a certain point in the vertical canopy profile. In the present study, GLI was used as a measure of light transmission. To estimate the GLI for each sap flux tree, a synthetic hemispherical photograph (SHP) was generated at the respective crown centre and at the respective maximum tree height. For this analysis, the entire point clouds of the study plots including their surroundings were used. We applied the method by Moeser et al. (2014) for producing SHPs from point clouds, therein closely following Brüllhardt et al. (2020) in deriving the point clouds photogrammetrically from the SfM technique. A searching radius of 100 m as suggested by Moeser et al. (2014) was chosen, that is, all points within a horizontal distance of less than 100 m to the origin (i.e., the position of the virtual camera) were considered. After running exemplary tests with different configurations, satisfactory results (as compared to visual assessments) were achieved with the size of 2 pixels for the nearest point and 0.2 pixels for the most distant element. The SHPs were then used to estimate gap light index above every target tree, wherein errors were produced for three trees, leading to a reduced sample size of 39 trees for the GLI analysis. The calculation of the GLI based on SHPs was carried out using *Hemisfer* 2.2 (Schleppi et al., 2007; Thimonier et al., 2010), which was designed for estimating light regime from SHPs. For this analysis, the input SHP has to be transformed into a black-and-white picture by classifying each pixel as sky or canopy element based on a brightness threshold; therein, *Hemisfer* 2.2 allows the automatic calculation of the optimal threshold using an algorithm for separating canopy and sky by edge detection (Nobis & Hunziker, 2005). The obtained black-and-white picture is then used as a mask that determines the amount of incident light transmitted through canopy elements. Following the default setting of *Hemisfer* 2.2, atmospheric transmissions of 40% and 20% were used for direct radiation and diffuse radiation, respectively.

As another variable related to crown exposure and light availability of single trees, we calculated the relative tree height of all sap flux trees. Therein, the maximum z-value within a given crown was divided by the maximum z-value within the plot point cloud. An overview of the exposure-related variables and their calculation can be found in Table S1.

2.4 | Statistical analysis

For an initial examination of potential relationships between the 21 variables in our dataset (six target variables related to transpiration and 15 potential predictors, see Table S1), we calculated a correlation

matrix (Figure S3) using the *corrplot* library (Wei & Simko, 2021). To account for potential non-linear relationships, we also calculated a correlation matrix after natural log transformation of all variables (Figure S4).

Linear regressions were applied to analyse the relationships between per-tree transpiration and variables in the categories crown dimension, crown shape, crown leaf density and crown exposure (Table S1). Where more than one model was significant ($P < 0.05$) within a given category, R^2, Akaike's Information Criteria (AIC) and Bayesian Information Criteria (BIC) were compared, and the best performing models were presented. Residual plot analysis with visual examinations for normality and homoscedasticity gave no indications of non-linearity for per-tree transpiration and thus the data were not transformed. In contrast, the examined transpiration rates per unit crown dimension (or LAD) and the according predictors were natural log transformed. On the scale of the raw data, fitting a log–log linear regression model corresponds to a power-law relationship.

To further explain observed variance in per-tree transpiration rates, we applied multiple linear regression models combining the best performing crown dimension-related metrics with the best performing variables within the categories crown shape, crown leaf density and crown exposure. Due to the limited sample size of 42 sap flux trees, a maximum of two predictors were used in the multiple regression models. The correlation matrix and variance inflation factors were used to check for multicollinearity (Vatcheva et al., 2016). Therein, only variable pairs for which the correlation coefficient was below 0.6 were used in the multiple models. Each model was tested in two versions, first as an additive model ($y \sim x_1 + x_2$) and secondly including interaction between variables ($y \sim x_1 \times x_2$). In our study, we present multiple models that fulfil the following criteria: (1) overall model significance ($P < 0.05$), (2) variable significance ($P < 0.05$) for both variables in additive models and for at least the interaction term in models with variable interaction and (3) more of the observed variance in transpiration rates explained than in the respective simple regression models. Where more than one multiple model fulfilled all criteria within a given category, the best performing model (in terms of R^2, AIC and BIC) was presented. To visualize the results of the multiple regression models, we computed partial predictions for selected predictors along their respective observed ranges while keeping the second predictor at its median, minimum and maximum value, respectively. The analysis of transpiration per unit crown dimension (and per unit LAD) with multiple regression models was carried out in analogy to the analysis of per-tree transpiration, but with natural log transformed target variables and predictors. For all statistical analyses and graphing, R 4.0.0 (R Core Team, 2020) was used.

3 | RESULTS

3.1 | Per-tree transpiration

Among 15 potential predictors (Tables S1 and S2) variables of crown dimension explained most (46%–68%) of the observed variance in daily per-tree transpiration in linear regression models, therein consistently indicating increasing transpiration with increasing crown dimension (Table S3). The baseline predictor was crown volume ($R^2 = 0.63$, $P < 0.001$, Figure 3a) as presented in a previous study (Ahongshangbam et al., 2020; note: value of one tree corrected in the present study). Two crown dimension-related variables performed better than crown volume as single predictors, crown surface area ($R^2 = 0.64$, $P < 0.001$, Figure 3b) and crown volume of the upper crown half ($R^2 = 0.68$, $P < 0.001$, Figure 3c). The crown dimension-related metrics were correlated among each other, while there were no close correlations ($R < 0.6$) between crown dimension and any variables in the categories crown shape, leaf density or exposure (Figure S3). The best performing predictors in these three categories explained far less of the variance in per-tree transpiration than crown dimension, 8% with crown top-heaviness ($P < 0.05$, Figure 3d), 11% with leaf area index (LAI) ($P < 0.05$, Figure 3e) and 20% with gap light index (GLI) ($P < 0.01$, Figure 3f), respectively.

Multiple linear regressions explained more of the variance in per-tree transpiration than the simple regression models when using the crown dimension variable crown volume in interaction with the respective best-performing variables of crown shape, leaf density or exposure (Table S4). As such, 74% of variance were explained by the interaction of crown volume with crown top-heaviness ($P < 0.001$, Figure 4a), 69% by the interaction with LAI ($P < 0.001$, Figure 4b) and 68% by the interaction with GLI ($P < 0.001$, Figure 4c). All three models have a significant interaction term which suggests that the positive effects of crown top-heaviness, LAI and GLI on per-tree transpiration increase with increasing crown dimension (Figure 4, Figure S5). At the maximum crown volume in our study (approx. 1500 m^3), variations between the respective observed minima and maxima in top-heaviness, LAI and GLI induce 2.3- to 3.3-fold differences in per-tree transpiration.

3.2 | Transpiration per unit crown dimension

Transpiration rates per unit crown dimension were assessed with log–log linear regression models using different variables (Tables S5 to S8). All models suggest relatively low and almost constant transpiration per unit crown dimension for medium-sized and large crowns, while small crowns have higher transpiration rates. Crown volume of the upper crown half performed best as a single predictor of transpiration per unit crown dimension ($R^2 = 0.74$, $P < 0.001$, Figure 5a), followed by crown volume ($R^2 = 0.69$, $P < 0.001$, Figure 5b). Applying multiple linear regression models only slightly further increased the explained variance, with crown volume of the upper crown half and stem diameter as interacting predictors ($R^2 = 0.76$, $P < 0.001$, Figure S6a).

We further assessed transpiration per unit leaf area density (LAD, Table S9). The model suggests a similar pattern as for transpiration per unit crown dimension, that is, higher transpiration per unit LAD in crowns with low LAD and lower transpiration rates for

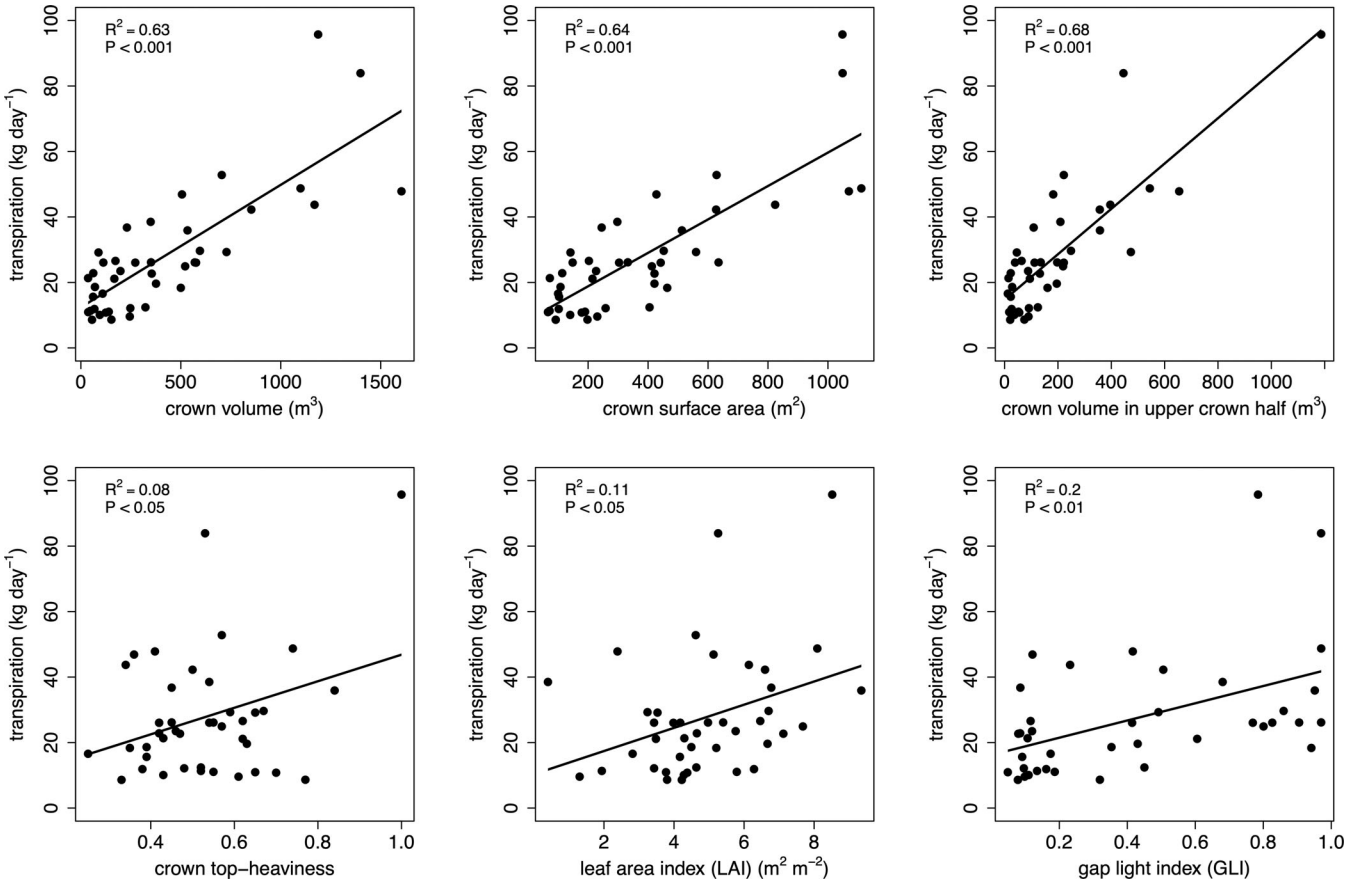

FIGURE 3 Per-tree transpiration of 42 clearly identified sap flux trees versus variables derived from 3D point cloud analyses. The depicted predictors are the three best performing within the category crown-dimension related variables, with crown volume (a), crown surface area (b) and crown volume in the upper crown half (c), and the best performing within the categories crown shape (crown top-heaviness, d), crown leaf-density variables (leaf area index, e) and light exposure-related variables (gap light index, f). The lines are the predictions of linear regression models.

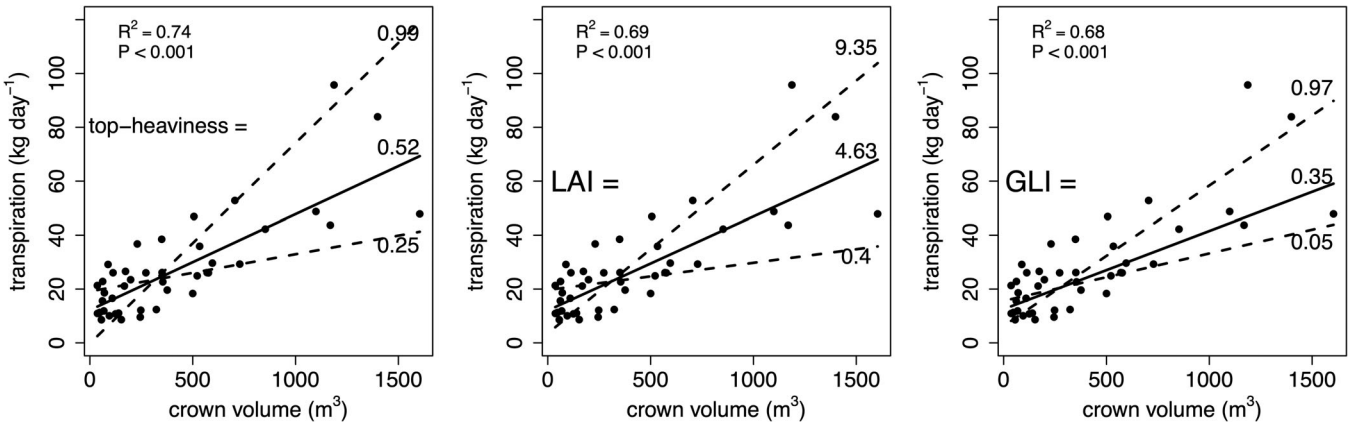

FIGURE 4 Per-tree transpiration vs. crown volume (black dots) and predictions of multiple linear regression models using crown volume in interaction with crown top-heaviness (a), leaf area index (LAI, b) and gap light index (GLI, c). The solid lines are partial predictions at median crown top-heaviness (unitless), LAI ($m^2\ m^{-2}$) and GLI (unitless), the dashed lines are partial predictions using the respective minimum and maximum values of top-heaviness, LAI and GLI as observed among the 42 sap flux trees. Minimum, median and maximum values of top-heaviness (a), LAI (b) and GLI (c) are depicted next to the prediction lines.

medium-density and high-density crowns ($R^2 = 0.62$, $P < 0.001$, Figure 5c). The considerable scatter observed among medium-density crowns is largely explained when applying a multiple regression model with the predictors LAD and crown volume ($R^2 = 0.8$, $P < 0.001$, Figure S6b,c). Therein, at a given LAD, the transpiration predicted for large crowns is higher than for small

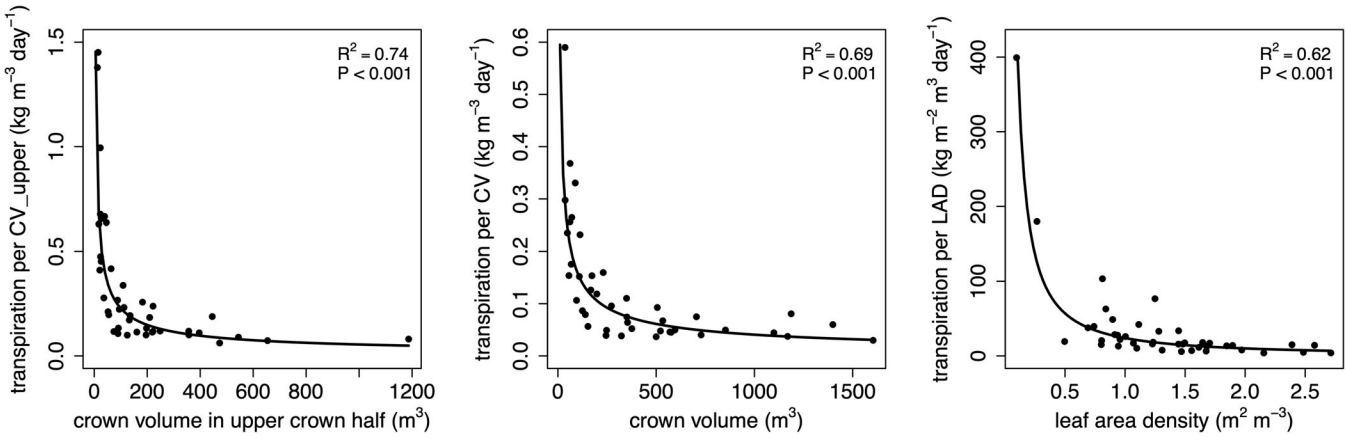

FIGURE 5 Transpiration rates per unit crown volume in the upper crown half (CV_upper), per unit total crown volume (CV) and per unit leaf area density (LAD), plotted vs. crown volume in the upper crown half (a), crown volume (b) and leaf area density (c), respectively. The lines are the predictions of log–log linear regression models.

crowns; the effects are additive, that is, no significant interaction among the predictors was observed (Table S4).

4 | DISCUSSION

For the studied tropical rainforest, UAV imagery-derived canopy structures well predicted tree transpiration rates. As a single variable crown dimension was most influential, with further enhancing effects of crown shape, leaf density and light exposure. Combinations of two predictor variables explained up to 74% of the observed variance in per-tree transpiration, up to 76% in transpiration per unit crown dimension and up to 80% per unit leaf area density. To our best knowledge, this is the first study using 3D point clouds in such a complex vegetation type for predicting transpiration.

4.1 | Methodological considerations

We applied the TDP sap flux method for estimating tree transpiration. The range in per-tree transpiration rates observed in our study falls within the range reported in a global review study across 67 tree species in 35 genera, where 90% of transpiration estimates were between 10 and 200 kg day^{-1} (Wullschleger et al., 1998). The range and our overall mean (28.9 kg day^{-1}) also conform to more recent studies in tropical rainforests (Dierick & Hölscher, 2009; Kotowska et al., 2021; Röll et al., 2019).

From the simultaneously carried out drone RGB imaging campaigns, dense point clouds were created with the well-established SfM technique (Iglhaut et al., 2019; Lowe, 2004). The point clouds represented the forest canopy in high detail and the derived orthomosaics allowed for the manual delineation of individual tree crowns, in our case of the sap flux trees with known locations, characteristics and surroundings. Even though only dominant and co-dominant trees with access to the upper canopy layers had been chosen as sap flux trees, less than 60% of the trees were clearly identified in the aerial images due to the high density of tree crowns and multi-layered structure of the canopy. For future studies in equally dense and complex (forest) ecosystems, pre-selecting the sap flux trees from the orthomosaics, marking their canopies or applying high-precision georeferencing (e.g., via real time kinematics) for both drone imaging and ground crown mapping is recommended.

For estimating crown leaf density variables of each sample tree from the crown point clouds, we followed de Almeida et al. (2019) to derive LAI estimates. The methodology is commonly applied for LiDAR based point clouds (e.g., de Almeida et al., 2019; Richardson et al., 2009; Zhao & Popescu, 2009), but is expected to work just as well with any type of point cloud of sufficient density, for example, derived from photogrammetry and the SfM technique (Comba et al., 2020). Previous studies reported good agreement between aerial RGB and LiDAR-derived point clouds for crown analyses (Guerra-Hernández et al., 2018; Thiel & Schmullius, 2017). From the variable LAI, we further calculated LAD and the total leaf area per tree (Table S1). We further used the point clouds to generate synthetic hemispherical photographs (SHPs), which were reported to produce accurate estimates of canopy closure and plant area index compared to actual hemispherical photographs in a previous study (Moeser et al., 2014). SHPs taken at the top of a given tree via a virtual camera can be used to estimate light availability (Cifuentes et al., 2017; Van der Zande et al., 2011), for which we employed the gap light index (GLI, Canham, 1988) in our study. We therein closely followed Brüllhardt et al. (2020), who had concluded that SHPs generated from photogrammetry-based point clouds work very well for estimating small-scale light transmission.

4.2 | Controls of per-tree transpiration

The crown dimension-related metrics crown volume, crown surface area and crown volume in the upper crown half are the most

influential single structural variables on per-tree transpiration that have been identified in the studied rainforest so far. Among the 42 studied trees, they explained 63% to 68% of the observed variance in transpiration. Two commonly applied variables in previous studies, ground projection area and total leaf area per tree, explained substantially less (58% and 52%, respectively) of the observed variance in our study ($P < 0.001$, see Figure S7a,b). Several of the studied crown dimension metrics explained more of the variance than DBH (37%) as a broadly applied baseline predictor for per-tree transpiration (e.g., Dierick & Hölscher, 2009; Kotowska et al., 2021; Meinzer et al., 2001, 2005; Vertessy et al., 1995; Wang et al., 2019; Yue et al., 2008). Our results add to previous studies showing that per-tree transpiration often scales linearly with crown dimension (Ahongshangbam et al., 2019, 2020; Hatton et al., 1998; Palmer et al., 2009; Radersma et al., 2006; Sala et al., 1996; Santiago et al., 2000; Vertessy et al., 1997). Crown dimension to some extent likely already integrates tree responses to different environmental conditions and probably also to competition among trees.

The studied variables of crown shape, leaf density and exposure explained less than 21% of the variance in per-tree transpiration when applied as single predictors. The only variable of crown shape that had a significant relationship with transpiration was crown top-heaviness. The model, despite very low explanatory power, suggests that per-tree transpiration is more than two-times higher for crowns with a top-heavy shape than for bottom-heavy crowns. In general, studies relating tree transpiration to the crown shape of single trees are rare. One previous study reported higher per-tree transpiration rates when intra-canopy heterogeneity was maximized within a given space compared to uniform crowns (Bauerle et al., 2004). In contrast, in our study we did not find a significant relationship between per-tree transpiration and canopy roughness length, a variable that characterizes the heterogeneity of the crown surface.

Regarding variables of leaf density, LAI had a significant relationship with per-tree transpiration; the model suggests a doubling of transpiration rates from approx. 20 to 40 kg day^{-1} as the LAI increases four-fold from approx. 2 to 8 m^2 m^{-2}. Even though the model has rather low explanatory power, it is within expectation. In general, LAI is often incorporated into models at the stand-scale, wherein up to a certain threshold higher LAI leads to higher (evapo) transpiration (e.g., Birhanu et al., 2019; Farid et al., 2008; Wang et al., 2014). At the scale of single trees, rather than LAI the total leaf area per tree is often applied as a predictor of per-tree transpiration; in our study, we considered the total leaf area per tree a variable of crown dimension (see above) due to its dependence on ground projection area in its calculation, and due to its close correlation with the other crown dimension metrics.

Regarding the variables of crown exposure, per-tree transpiration significantly increased with increasing relative tree height and increasing GLI. Therein, transpiration more than doubled from low to high GLI. Direction and effect size were in line with our initial expectations, but as for the crown shape and leaf density variables, the variance explained by GLI as a single predictor was low. In line with our results, previous studies also found significant effects of radiation-related variables on tree transpiration (e.g., Dierick & Hölscher, 2009; Kunert et al., 2010; Oren & Pataki, 2001). However, studies that quantify the light availability of co-occurring trees with different canopy positions within a stand are rare due to the complexity of assessing the light availability at the top of crowns. One previous study from a subtropical mixed forest in Chongqing (Zhang et al., 2019) reported a negative correlation between per-tree transpiration of reference trees and an index characterizing the dominance of nearest neighbours, indicating that large-sized trees with low competition pressure and high light availability had the highest transpiration. Observations from coffee and cacao agroforestry systems where the shade tolerant crops are cultivated under varying tree cover revealed opposite patterns, that is, increasing per-tree transpiration with decreasing canopy gap fraction (Köhler et al., 2009; van Kanten & Vaast, 2006). The relatively low explained variance by GLI in our study may be caused by the co-existence of plants with different shade-tolerance. In the diverse stands of the Harapan rainforest (201 tree species on four plots covering a total of 1 ha, Rembold et al., 2017), tree species that differ in their transpiration responses to light likely co-occur, and GLI alone therefore only has moderate power in explaining tree-to-tree variations in transpiration rates.

Even for the best performing crown dimension-related predictors, we observed considerable scatter in the relationship with per-tree transpiration at a given crown dimension. We applied multiple regression models to examine whether adding variables of crown shape, leaf density or light exposure as predictors reduces unexplained variance in transpiration. The three variables analysed more closely in our study, crown topheaviness (crown shape), LAI (leaf density) and GLI (light exposure) each interacted significantly with crown volume in multiple linear regression models, explaining 68% to 74% of the variance in per-tree transpiration as compared to 63% when using crown volume alone. The models indicate that the marginal effects of a top-heavy crown shape, LAI and GLI increase with increasing crown dimension, that is, crown dimension has a dominant role for predicting per-tree transpiration of small- and medium-sized crowns, but shape, leaf density and exposure of crowns induce substantial variability into the transpiration rates of (very) large crowns. While trees with small crowns mostly occur at lower positions in the canopy, trees that have larger crowns generally take up higher strata. Differently positioned crowns within the forest canopy experience varying environmental conditions and adapt their crown shape, leaf density and light response accordingly, which influences their individual transpiration rates (e.g., Givnish, 1988; Lei & Lechowicz, 1990; Schulze et al., 2019). Integrating such tree-level variables into the prediction of per-tree transpiration helped to explain tree-to-tree variation that was not explained by (crown) dimension-related variables alone. Likewise, a previous study found that uncertainties in the scaling of crown dimensions from simple biometric predictors such as tree diameter and height were significantly reduced by including information on environmental context such as local light and water availability (Shenkin et al., 2020).

4.3 | Transpiration per unit crown dimension

We found high transpiration rates per unit crown dimension for small crowns, and relatively low and almost constant rates for medium-sized and large crowns. Log–log linear regression models explained up to 74% of the variance in transpiration per unit crown dimension, wherein variables related to crown volume performed best. To our knowledge, no previous (rain)forest studies are available for a comparison of observed magnitude and patterns of transpiration per unit crown volume. Specifically at the stand-level, but also at the level of single trees, transpiration is often expressed per unit ground (projection) area, commonly denoted in mm day^{-1}. As for transpiration per unit crown volume, transpiration per unit ground area tended to be higher (0.3–1.5 mm day^{-1}) for trees with small crowns than medium and large-sized crowns (0.2–0.5 mm day^{-1}), but the explanatory power of the model was relatively low compared to other crown-dimension variables ($R^2 = 0.32$, $P < 0.001$, Figure S7c). While no studies from tropical rainforests are available for a comparison to our results, previous studies in the tropics covered agroforests, a secondary forest patch and a reforestation stand, where crown projection areas were generally smaller than in our study (min. 14 m^2, mean 84 m^2, max. 216 m^2, Table S1). For the shade-tolerant understory crop cacao (*Theobroma cacao*) and the light-demanding shade tree species *Gliricidia sepium* in an agroforest in Indonesia, transpiration per unit ground area was reported to be 0.5–0.6 mm day^{-1} (cacao) and 0.2–0.5 mm day^{-1} (*G. sepium*) (Köhler et al., 2009), with average crown projection areas of 20.2 m^2 (cacao) and 40.4 m^2 (*G. sepium*). For young coffee agroforestry shade tree species in Costa Rica with relatively small crowns, transpiration rates of 0.4 to 1.1 mm day^{-1} were reported for *Eucalyptus deglupta*, 0.7 to 2.1 mm day^{-1} for *Terminalia ivorensis* and 0.1 to 0.8 mm day^{-1} for *Erythrina poeppigiana* (Van Kanten and Vaast, 2006). In a secondary forest patch in Vietnam, transpiration was between 0.4 and 1.5 mm day^{-1} for trees with relatively small crowns (13–60 m^2). Even smaller-crowned trees (13–32 m^2) at the edge of the forest patch generally had much higher transpiration rates of up to 2.9 mm day^{-1} (Giambelluca et al., 2003). A study in 12-year old reforestation stands in the Philippines reported transpiration rates between 0.6 and 1.9 mm day^{-1} across 10 different species (Dierick & Hölscher, 2009), also with relatively small crown dimensions (7–32 m^2). For the range of crown dimensions covered in these studies (<60 m^2), we observed transpiration rates per unit ground area between 0.3 and 1.5 mm day^{-1}, that is, a comparable but overall lower range with substantial tree-to-tree variation. This finding seems reasonable in the context of the high structural and functional diversity and the associated complex interactions in tropical rainforests. As such, the high competition for light in the densely packed, multistoried canopy layers, along with the generally high competition for space and resources at the high stand densities observed in lowland rainforests in the study region (>500 trees ha^{-1} with a DBH of at least 10 cm), may result in on average lower transpiration per unit ground area than in less complex ecosystems. In accordance with this line of argument, minimizing competition experimentally in open-grown, isolated *Acer saccharum* trees with permanent access to groundwater (notably, in temperate North America) lead to very high transpiration rates per unit ground area (2.5–7 mm day^{-1}, Dawson, 1996); another reason for these high values may be the long day length during northern hemisphere summer.

Transpiration per unit leaf area has also been the subject of some previous studies. In our study, the explanatory power of the model was intermediate compared to other crown-dimension related variables ($R^2 = 0.62$, $P < 0.001$, Figure S7d). In accordance with the previous results, the model predicts higher transpiration per unit leaf area (>0.1 kg m^{-2} day^{-1}) for small crowns (<100 m^2 leaf area) and lower and relatively constant rates for larger crowns (~0.1 kg m^{-2} day^{-1}). Our estimates for rainforest tree species are mostly much lower than reported in a global review study for several fast growing (plantation) species like *Eucalyptus* (0.1–8.5 kg m^{-2} day^{-1}), *Pinus* (0.6–1.2 kg m^{-2} day^{-1}), *Populus* (4.2 kg m^{-2} day^{-1}) and *Salix* (2.7 to 3.8 kg m^{-2} day^{-1}) (Wullschleger et al., 1998). Much higher rates than in our study were also reported for single standing *Alnus* and *Tilia* street trees in Helsinki (0.8–1.1 kg m^{-2} day^{-1}) (Riikonen et al., 2016). For the previously mentioned agroforestry species in Sulawesi, cacao and *G. sepium*, transpiration rates per unit leaf area were approx. 0.3 and 0.2 kg m^2 day^{-1}, at average total leaf areas of 34 and 57 m^2, respectively (Köhler et al., 2009). The reported rates correspond well to our results, that is, when inputting the respective crown dimensions into our model (Figure S7d) it predicts identical transpiration rates per unit leaf area of 0.3 and 0.2 kg m^2 day^{-1}, respectively. For the shade tolerant species coffee, it was found that sun-exposed plants had higher transpiration rates per unit leaf area than coffee grown under shade, but the reverse was observed when transpiration was expressed per unit ground area (van Kanten & Vaast, 2006). For different dryland tree species in parklands in Senegal, more than fourfold differences in transpiration per unit leaf area were reported for relatively small trees (17 to 52 m^2 leaf area), along with substantial seasonal variability, with transpiration rates of approx. 1.0 to 2.0 kg m^2 day^{-1} at the beginning and 0.3 to 1.0 kg m^2 day^{-1} at the end of the dry season (Deans & Munro, 2004). For similarly small trees (1 to 28 m^2 leaf area) of three species in tree lines in sub-humid Kenya, rates between 0.3 and 1.0 kg m^2 day^{-1} were reported, wherein transpiration rates per unit leaf area were (slightly) enhanced by phosphorus fertilization (Radersma et al., 2006). For 24 relatively small *Metrosideros polymorpha* trees across six study sites in montane cloud forest stands in Hawaii, transpiration per unit leaf area was reported to be higher than in our study (>0.34 kg m^{-2} day^{-1}) and highly variable among sites, with on average 63% higher rates on level, waterlogged, open-canopy sites (<1.3 m^2 m^{-2} LAI) than on sloped closed-canopy sites (>5.1 m^2 m^{-2} LAI) (Santiago et al., 2000). Overall, the range in transpiration per unit leaf area as observed for trees with a small total leaf area in our study (~0.1–1.2 kg m^2 day^{-1}) is comparable but lower than the values reported in previous studies. To our knowledge, there are no studies on large tropical (rainforest) trees for a comparison of magnitude and patterns in transpiration rates per unit leaf area. However, one study on *Pinus ponderosa* in North America reported 53% lower transpiration per unit leaf area in old trees (250 years old, 30 m tall) compared to young

trees (40 years old, 10 m tall) due to deceasing hydraulic conductance with advancing tree age (Hubbard et al., 1999). In our study in a tropical rainforest, similar mechanisms may explain the observed decrease in transpiration per unit leaf area with increasing crown dimension.

We further assessed transpiration per unit leaf area density (LAD, Table S9), that is, transpiration normalized to one m^2 of leaf area per m^3 of crown volume. The model suggests a similar pattern as for transpiration per unit crown dimension, with high transpiration per unit LAD in crowns with low LAD and much lower rates for medium-density and high-density crowns ($R^2 = 0.62$, $P < 0.001$, Figure 5c). Therein, the considerable scatter observed in transpiration rates of medium-density crowns was largely explained when applying multiple regression with the predictors LAD and crown volume ($R^2 = 0.8$, $P < 0.001$, Figure S6b,c, Table S4), wherein, at a given LAD, the transpiration per unit LAD predicted for large crowns was higher than for small crowns. To our knowledge, there are no previous studies assessing transpiration per unit LAD for comparison.

Transpiration rates per unit crown dimension (or per unit LAD) had thus far not been assessed for tropical rainforest trees across multiple sites and involving variably sized and vertically positioned tree crowns. Overall, there is a need for further studies untangling transpiration rates of rainforest trees and their drivers, for example, regarding the effects of competition, and thus close the gap in so far unexplained variability of rainforest tree transpiration. We consider our study a first step by contributing new insights on the dominant role of crown dimension for predicting (rainforest) tree transpiration. Our study demonstrates that 3D point cloud analysis is a very promising tool for better understanding (water) exchange processes of trees and other plants variably structured and positioned in the forest canopy, thus allowing for research that would be extremely challenging or impossible using conventional ground based methods. There is a great potential of the method for better linking forest structure and forest functions.

ACKNOWLEDGEMENTS

We would like to thank the Ministry of Research, Technology and Higher Education, Indonesia, for issuing the research permit for field work (No. 285/SIP/FRP/E5/Dit.KI/VIII/2016 and No. 322/SIP/FRP/E5/Dit.KI/IX/2016). We would also like to thank our field assistant Erwin Pranata for supporting us during the field campaigns. Last but not least, we thank the reviewers for very constructive and helpful comments. Open Access funding enabled and organized by Projekt DEAL.

FUNDING INFORMATION

This study was financially supported by the Deutsche Forschungsgemeinschaft (DFG) in the framework of a collaborative German–Indonesian research project (CRC 990 'EFForTS' project: sub-project A02), which is gratefully acknowledged.

CONFLICT OF INTEREST STATEMENT

The authors declare no conflicts of interest.

DATA AVAILABILITY STATEMENT

The data that support the findings of this study are available from the corresponding author upon request. They are permanently stored in the data repository of the University of Göttingen "GRO.data" and become available at https://doi.org/10.25625/VPGDWE once the study is published. This includes the R code applied for the analysis.

ORCID

Alexander Röll https://orcid.org/0000-0001-9457-4459
Peter Hahn https://orcid.org/0000-0001-8867-0006

REFERENCES

Agisoft LLC. (2019). AgiSoft PhotoScan Professional (Version 1.2.6) (Software). http://www.agisoft.com/downloads/installer/

Ahongshangbam, J., Khokthong, W., Ellsäßer, F., Hendrayanto, H., Hölscher, D., & Röll, A. (2019). Drone-based photogrammetry-derived crown metrics for predicting tree and oil palm water use. *Ecohydrology*, *12*(6), e2115. https://doi.org/10.1002/eco.2115

Ahongshangbam, J., Röll, A., Ellsäßer, F., Hendrayanto, & Hölscher, D. (2020). Airborne tree crown detection for predicting spatial heterogeneity of canopy transpiration in a tropical rainforest. *Remote Sensing*, *12*(4), 651. https://doi.org/10.3390/rs12040651

Aparecido, L. M., Miller, G. R., Cahill, A. T., & Moore, G. W. (2016). Comparison of tree transpiration under wet and dry canopy conditions in a Costa Rican premontane tropical forest. *Hydrological Processes*, *30*(26), 5000–5011.

Bauerle, W. L., Bowden, J. D., McLeod, M. F., & Toler, J. E. (2004). Modeling intra-crown and intra-canopy interactions in red maple: Assessment of light transfer on carbon dioxide and water vapor exchange. *Tree Physiology*, *24*(5), 589–597.

Birhanu, D., Kim, H., & Jang, C. (2019). Effectiveness of introducing crop coefficient and leaf area index to enhance evapotranspiration simulations in hydrologic models. *Hydrological Processes*, *33*(16), 2206–2226.

Brüllhardt, M., Rotach, P., Schleppi, P., & Bugmann, H. (2020). Vertical light transmission profiles in structured mixed deciduous forest canopies assessed by UAV-based hemispherical photography and photogrammetric vegetation height models. *Agricultural and Forest Meteorology*, *281*, 107843. https://doi.org/10.1016/j.agrformet.2019.107843

Canham, C. D. (1988). An index for understory light levels in and around canopy gaps. *Ecology*, *69*(5), 1634–1638. https://doi.org/10.2307/1941664

Cifuentes, R., Van der Zande, D., Salas, C., Tits, L., Farifteh, J., & Coppin, P. (2017). Modeling 3D canopy structure and transmitted PAR using terrestrial LiDAR. *Canadian Journal of Remote Sensing*, *43*(2), 124–139. https://doi.org/10.1080/07038992.2017.1286937

CloudCompare. (2019). CloudCompare (version 2.11.1) [GPL software]. http://www.cloudcompare.org/

Comba, L., Biglia, A., Ricauda Aimonino, D., Tortia, C., Mania, E., Guidoni, S., & Gay, P. (2020). Leaf Area Index evaluation in vineyards using 3D point clouds from UAV imagery. *Precision Agriculture*, *21*(4), 881–896. https://doi.org/10.1007/s11119-019-09699-x

Dawson, T. E. (1996). Determining water use by trees and forests from isotopic, energy balance and transpiration analyses: The roles of tree size and hydraulic lift. *Tree Physiology*, *16*(1–2), 263–272.

de Almeida, D. R. A., Stark, S. C., Shao, G., Schietti, J., Nelson, B. W., Silva, C. A., Gorgens, E. B., Valbuena, R., de Almeida Papa, D., & Brancalion, P. H. S. (2019). Optimizing the remote detection of tropical rainforest structure with airborne LiDAR: Leaf area profile sensitivity to pulse density and spatial sampling. *Remote Sensing*, *11*(1), 92. https://doi.org/10.3390/rs11010092

Deans, J. D., & Munro, R. C. (2004). Comparative water use by dryland trees in Parklands in Senegal. *Agroforestry Systems*, *60*(1), 27–38.

Dierick, D., & Hölscher, D. (2009). Species-specific tree water use characteristics in reforestation stands in the Philippines. *Agricultural and Forest Meteorology*, *149*(8), 1317–1326. https://doi.org/10.1016/j.agrformet.2009.03.003

Dietmaier, A., McDermid, G. J., Rahman, M. M., Linke, J., & Ludwig, R. (2019). Comparison of LiDAR and digital aerial photogrammetry for characterizing canopy openings in the boreal forest of northern Alberta. *Remote Sensing*, *11*(16), 1919. https://doi.org/10.3390/rs11161919

Drescher, J., Rembold, K., Allen, K., Beckschäfer, P., Buchori, D., Clough, Y., Faust, H., Fauzi, A. M., Gunawan, D., Hertel, D., Irawan, B., Jaya, I. N. S., Klarner, B., Kleinn, C., Knohl, A., Kotowska, M. M., Krashevska, V., Krishna, V., Leuschner, C., … Scheu, S. (2016). Ecological and socio-economic functions across tropical land use systems after rainforest conversion. *Philosophical Transactions of the Royal Society B: Biological Sciences*, *371*(1694), 20150275. https://doi.org/10.1098/rstb.2015.0275

Ellison, D., Morris, C. E., Locatelli, B., Sheil, D., Cohen, J., Murdiyarso, D., Gutierrez, V., van Noordwijk, M., Creed, I. F., Pokorny, J., Gaveau, D., Spracklen, D. V., Tobella, A. B., Ilstedt, U., Teuling, A. J., Gebrehiwot, S. G., Sands, D. C., Muys, B., Verbist, B., … Sullivan, C. A. (2017). Trees, forests and water: Cool insights for a hot world. *Global Environmental Change*, *43*, 51–61. https://doi.org/10.1016/j.gloenvcha.2017.01.002

Ewers, B. E., Mackay, D. S., Gower, S. T., Ahl, D. E., Burrows, S. N., & Samanta, S. S. (2002). Tree species effects on stand transpiration in northern Wisconsin. *Water Resources Research*, *38*(7), 8-1.

Farid, A., Goodrich, D. C., Bryant, R., & Sorooshian, S. (2008). Using airborne lidar to predict Leaf Area Index in cottonwood trees and refine riparian water-use estimates. *Journal of Arid Environments*, *72*(1), 1–5.

Fisher, J. B., Malhi, Y., Bonal, D., Da Rocha, H. R., De Araújo, A. C., Gamo, M., Goulden, M. L., Hirano, T., Huete, A. R., Kondo, H., Kumagai, T., Loescher, H. W., Miller, S., Nobre, A. D., Nouvellon, Y., Oberbauer, S. F., Panuthai, S., Roupsard, O., Saleska, S., … Von Randow, C. (2009). The land–atmosphere water flux in the tropics: The land-atmosphere water flux in the tropics. *Global Change Biology*, *15*(11), 2694–2714. https://doi.org/10.1111/j.1365-2486.2008.01813.x

Giambelluca, T. W., Ziegler, A. D., Nullet, M. A., Truong, D. M., & Tran, L. T. (2003). Transpiration in a small tropical forest patch. *Agricultural and Forest Meteorology*, *117*(1–2), 1–22. https://doi.org/10.1016/S0168-1923(03)00041-8

Givnish, T. (1988). Adaptation to sun and shade: A whole-plant perspective. *Functional Plant Biology*, *15*(2), 63. https://doi.org/10.1071/PP9880063

Granier, A. (1985). Une nouvelle méthode pour la mesure du flux de sève brute dans le tronc des arbres. *Annales des Sciences Forestières*, *42*(2), 193–200. https://doi.org/10.1051/forest:19850204

Guerra-Hernández, J., Cosenza, D. N., Rodriguez, L. C. E., Silva, M., Tomé, M., Díaz-Varela, R. A., & González-Ferreiro, E. (2018). Comparison of ALS- and UAV(SfM)-derived high-density point clouds for individual tree detection in Eucalyptus plantations. *International Journal of Remote Sensing*, *39*(15–16), 5211–5235. https://doi.org/10.1080/01431161.2018.1486519

Hardanto, A., Röll, A., Niu, F., Meijide, A., Hendrayanto, & Hölscher, D. (2017). Oil palm and rubber tree wateruse patterns: Effects of topography and flooding. *Frontiers in Plant Science*, *8*, 452. https://doi.org/10.3389/fpls.2017.00452

Harja, D., Vincent, G., Mulia, R., & van Noordwijk, M. (2012). Tree shape plasticity in relation to crown exposure. *Trees*, *26*(4), 1275–1285. https://doi.org/10.1007/s00468-012-0703-x

Harrison, R. D., & Swinfield, T. (2015). Restoration of logged humid tropical forests: An experimental programme at Harapan Rainforest, Indonesia. *Tropical Conservation Science*, *8*(1), 4–16. https://doi.org/10.1177/194008291500800103

Hatton, T., Reece, P., Taylor, P., & McEwan, K. (1998). Does leaf water efficiency vary among eucalypts in water-limited environments? *Tree Physiology*, *18*(8–9), 529–536. https://doi.org/10.1093/treephys/18.8-9.529

Hu, L., & Zhu, J. (2008). Improving gap light index (GLI) to quickly calculate gap coordinates. *Canadian Journal of Forest Research*, *38*(9), 2337–2347. https://doi.org/10.1139/X08-073

Hubbard, R. M., Bond, B. J., & Ryan, M. G. (1999). Evidence that hydraulic conductance limits photosynthesis in old Pinus ponderosa trees. *Tree Physiology*, *19*(3), 165–172.

Iglhaut, J., Cabo, C., Puliti, S., Piermattei, L., O'Connor, J., & Rosette, J. (2019). Structure from motion photogrammetry in forestry: A review. *Current Forestry Reports*, *5*(3), 155–168. https://doi.org/10.1007/s40725-019-00094-3

Jarvis, P. G. (1976). The interpretation of the variations in leaf water potential and stomatal conductance found in canopies in the field. *Philosophical Transactions of the Royal Society of London. Series B, Biological Sciences*, *273*(927), 593–610.

Jordan, C. F., & Kline, J. R. (1977). Transpiration of trees in a tropical rainforest. *Journal of Applied Ecology*, *1*, 853–860.

Khokthong, W., Zemp, D. C., Irawan, B., Sundawati, L., Kreft, H., & Hölscher, D. (2019). Drone-based assessment of canopy cover for analyzing tree mortality in an oil palm agroforest. *Frontiers in Forests and Global Change*, *2*, 12. https://doi.org/10.3389/ffgc.2019.00012

Köhler, M., Dierick, D., Schwendenmann, L., & Hölscher, D. (2009). Water use characteristics of cacao and Gliricidia trees in an agroforest in Central Sulawesi. *Indonesia. Ecohydrology*, *2*(4), 520–529. https://doi.org/10.1002/eco.67

Kotowska, M. M., Link, R. M., Röll, A., Hertel, D., Hölscher, D., Waite, P.-A., Moser, G., Tjoa, A., Leuschner, C. & Schuldt, B. (2021). Effects of wood hydraulic properties on water use and productivity of tropical rainforest trees. *Frontiers in Forests and Global Change*, *3*, 598759.

Kunert, N., Aparecido, L. M., Higuchi, N., dos Santos, J., & Trumbore, S. (2015). Higher tree transpiration due to road-associated edge effects in a tropical moist lowland forest. *Agricultural and Forest Meteorology*, *213*, 183–192.

Kunert, N., Aparecido, L. M., Wolff, S., Higuchi, N., dos Santos, J., de Araujo, A. C., & Trumbore, S. (2017). A revised hydrological model for the Central Amazon: The importance of emergent canopy trees in the forest water budget. *Agricultural and Forest Meteorology*, *239*, 47–57.

Kunert, N., Schwendenmann, L., & Hölscher, D. (2010). Seasonal dynamics of tree sap flux and water use in nine species in Panamanian forest plantations. *Agricultural and Forest Meteorology*, *150*(3), 411–419. https://doi.org/10.1016/j.agrformet.2010.01.006

Lei, T. T., & Lechowicz, M. J. (1990). Shade adaptation and shade tolerance in saplings of three Acer species from eastern North America. *Oecologia*, *84*(2), 224–228. https://doi.org/10.1007/BF00318275

Lowe, D. G. (2004). Distinctive image features from scale-invariant keypoints. *International Journal of Computer Vision*, *60*(2), 91–110. https://doi.org/10.1023/B:VISI.0000029664.99615.94

McJannet, D., Fitch, P., Disher, M., & Wallace, J. (2007). Measurements of transpiration in four tropical rainforest types of north Queensland, Australia. *Hydrological Processes*, *21*(26), 3549–3564. https://doi.org/10.1002/hyp.6576

Meinzer, F. C., Bond, B. J., Warren, J. M., & Woodruff, D. R. (2005). Does water transport scale universally with tree size? *Functional Ecology*, *19*(4), 558–565. https://doi.org/10.1111/j.1365-2435.2005.01017.x

Meinzer, F. C., Goldstein, G., & Andrade, J. L. (2001). Regulation of water flux through tropical forest canopy trees: Do universal rules apply? *Tree Physiology*, *21*(1), 19–26. https://doi.org/10.1093/treephys/21.1.19

Moeser, D., Roubinek, J., Schleppi, P., Morsdorf, F., & Jonas, T. (2014). Canopy closure, LAI and radiation transfer from airborne LiDAR synthetic images. *Agricultural and Forest Meteorology*, *197*, 158–168. https://doi.org/10.1016/j.agrformet.2014.06.008

Nobis, M., & Hunziker, U. (2005). Automatic thresholding for hemispherical canopy-photographs based on edge detection. *Agricultural and Forest Meteorology*, *128*, 243–250. https://doi.org/10.1016/j.agrformet.2004.10.002

Oren, R., & Pataki, D. E. (2001). Transpiration in response to variation in microclimate and soil moisture in southeastern deciduous forests. *Oecologia*, *127*(4), 549–559. https://doi.org/10.1007/s004420000622

Palmer, A. R., Fuentes, S., Taylor, D., Macinnis-Ng, C., Zeppel, M., Yunusa, I., & Eamus, D. (2009). Towards a spatial understanding of water use of several land-cover classes: An examination of relationships amongst pre-dawn leaf water potential, vegetation water use, aridity and MODIS LAI. *Ecohydrology*, *3*, 1–10. https://doi.org/10.1002/eco.63

QGIS.org. (2020). QGIS geographic information system. Open Source Geospatial Foundation Project. http://qgis.org

R Core Team. (2020). R: A language and environment for statistical computing (4.0.0) (Software). R Foundation for Statistical Computing. http://www.R-project.org/

Radersma, S., Ong, C. K., & Coe, R. (2006). Water use of tree lines: Importance of leaf area and micrometeorology in sub-humid Kenya. *Agroforestry Systems*, *66*(3), 179–189.

Rembold, K., Mangopo, H., Tjitrosoedirdjo, S. S., & Kreft, H. (2017). Plant diversity, forest dependency, and alien plant invasions in tropical agricultural landscapes. *Biological Conservation*, *213*, 234–242. https://doi.org/10.1016/j.biocon.2017.07.020

Richardson, J. J., Moskal, L. M., & Kim, S.-H. (2009). Modeling approaches to estimate effective leaf area index from aerial discrete-return LIDAR. *Agricultural and Forest Meteorology*, *149*(6–7), 1152–1160. https://doi.org/10.1016/j.agrformet.2009.02.007

Riikonen, A., Järvi, L., & Nikinmaa, E. (2016). Environmental and crown related factors affecting street tree transpiration in Helsinki, Finland. *Urban Ecosystems*, *19*(4), 1693–1715.

Röll, A., Niu, F., Meijide, A., Ahongshangbam, J., Ehbrecht, M., Guillaume, T., Gunawan, D., Hardanto, A., Hendrayanto, Hertel, D., Kotowska, M. M., Kreft, H., Kuzyakov, Y., Leuschner, C., Nomura, M., Polle, A., Rembold, K., Sahner, J., Seidel, D., … Hölscher, D. (2019). Transpiration on the rebound in lowland Sumatra. *Agricultural and Forest Meteorology*, *274*, 160–171. https://doi.org/10.1016/j.agrformet.2019.04.017

Roussel, J. R., & Auty, D. (2018). LidR: Airborne LiDAR data manipulation and visualization for forestry applications, R Package Version 3.0.3. https://rdrr.io/cran/lidR/

Roxburgh, J. R., & Kelly, D. (1995). Uses and limitations of hemispherical photography for estimating forest light environments. *New Zealand Journal of Ecology*, *19*(2), 5.

Sala, A., Smith, S. D., & Devitt, D. A. (1996). Water use by Tamarix ramosissima and associated phreatophytes in a Mojave Desert floodplain. *Ecological Applications*, *6*(3), 888–898. https://doi.org/10.2307/2269492

Santiago, L. S., Goldstein, G., Meinzer, F. C., Fownes, J. H., & Mueller-Dombois, D. (2000). Transpiration and forest structure in relation to soil waterlogging in a Hawaiian montane cloud forest. *Tree Physiology*, *20*(10), 673–681.

Schleppi, P., Conedera, M., Sedivy, I., & Thimonier, A. (2007). Correcting non-linearity and slope effects in the estimation of the leaf area index of forests from hemispherical photographs. *Agricultural and Forest Meteorology*, *144*(3), 236–242. https://doi.org/10.1016/j.agrformet.2007.02.004

Schulze, E.-D., Beck, E., Buchmann, N., Clemens, S., Müller-Hohenstein, K., & Scherer-Lorenzen, M. (2019). *Plant ecology*. Springer.

Shenkin, A., Bentley, L. P., Oliveras, I., Salinas, N., Adu-Bredu, S., Marimon-Junior, B. H., Marimon, B. S., Peprah, T., Choque, E. L., Trujillo Rodriguez, L., Clemente Arenas, E. R., Adonteng, C., Seidu, J., Passos, F. B., Reis, S. M., Blonder, B., Silman, M., Enquist, B. J., Asner, G. P., & Malhi, Y. (2020). The influence of ecosystem and phylogeny on tropical tree crown size and shape. *Frontiers in Forests and Global Change*, *3*, 501757. https://doi.org/10.3389/ffgc.2020.501757

Silva, C. A., Crookston, N. L., Hudak, A. T., & Vierling, L. A. (2015). RLiDAR: An R package for Reading, processing and visualizing LiDAR (light detection and ranging) data, R Package Version 0.1. http://cran.rproject.org/web/packages/rLiDAR/index.html

Thiel, C., & Schmullius, C. (2017). Comparison of UAV photograph-based and airborne lidar-based point clouds over forest from a forestry application perspective. *International Journal of Remote Sensing*, *38*(8–10), 2411–2426. https://doi.org/10.1080/01431161.2016.1225181

Thimonier, A., Sedivy, I., & Schleppi, P. (2010). Estimating leaf area index in different types of mature forest stands in Switzerland: A comparison of methods. *European Journal of Forest Research*, *129*(4), 543–562. https://doi.org/10.1007/s10342-009-0353-8

Van der Zande, D., Stuckens, J., Verstraeten, W. W., Mereu, S., Muys, B., & Coppin, P. (2011). 3D modeling of light interception in heterogeneous forest canopies using ground-based LiDAR data. *International Journal of Applied Earth Observation and Geoinformation*, *13*(5), 792–800. https://doi.org/10.1016/j.jag.2011.05.005

van Kanten, R., & Vaast, P. (2006). Transpiration of arabica coffee and associated shade tree species in sub-optimal, low-altitude conditions of Costa Rica. *Agroforestry Systems*, *67*(2), 187–202. https://doi.org/10.1007/s10457-005-3744-y

Vatcheva, K., Lee, M., McCormick, J., & Rahbar, M. (2016). Multicollinearity in regression analyses conducted in epidemiologic studies. *Epidemiology Open Access*, *6*, 227. https://doi.org/10.4172/2161-1165.1000227

Vertessy, R. A., Benyon, R. G., O'Sullivan, S. K., & Gribben, P. R. (1995). Relationships between stem diameter, sapwood area, leaf area and transpiration in a young mountain ash forest. *Tree Physiology*, *15*(9), 559–567. https://doi.org/10.1093/treephys/15.9.559

Vertessy, R. A., Hatton, T. J., Reece, P., O'Sullivan, S. K., & Benyon, R. G. (1997). Estimating stand water use of large mountain ash trees and validation of the sap flow measurement technique. *Tree Physiology*, *17*(12), 747–756. https://doi.org/10.1093/treephys/17.12.747

Wallace, J., & McJannet, D. (2010). Processes controlling transpiration in the rainforests of north Queensland, Australia. *Journal of Hydrology*, *384*(1–2), 107–117. https://doi.org/10.1016/j.jhydrol.2010.01.015

Wallace, L., Lucieer, A., Malenovský, Z., Turner, D., & Vopěnka, P. (2016). Assessment of forest structure using two UAV techniques: A comparison of airborne laser scanning and structure from motion (SfM) point clouds. *Forests*, *7*(12), 62. https://doi.org/10.3390/f7030062

Wang, G., Shen, Y., Yang, X., Chen, Z., & Mo, B. (2019). Scaling up sap flow measurements from the stem scale to the individual scale for multi-branched Caragana korshinskii on the Chinese Loess Plateau. *Forests*, *10*(9), 785. https://doi.org/10.3390/f10090785

Wang, L., Good, S. P., & Caylor, K. K. (2014). Global synthesis of vegetation control on evapotranspiration partitioning. *Geophysical Research Letters.*, *41*(19), 6753–6757.

Wei, T., & Simko, V. (2021). R package 'corrplot': Visualization of a Correlation Matrix. (Version 0.92). https://github.com/taiyun/corrplot

Wullschleger, S. D., Meinzer, F. C., & Vertessy, R. A. (1998). A review of whole-plant water use studies in tree. *Tree Physiology*, *18*(8–9), 499–512.

Yue, G., Zhao, H., Zhang, T., Zhao, X., Niu, L., & Drake, S. (2008). Evaluation of water use of Caragana microphylla with the stem heat-balance method in Horqin Sandy Land, Inner Mongolia, China. *Agricultural and Forest Meteorology*, *148*(11), 1668–1678. https://doi.org/10.1016/j.agrformet.2008.05.019

Zhang, X., Wang, Y., Wang, Y., Zhang, S., & Zhao, X. (2019). Effects of social position and competition on tree transpiration of a natural mixed forest in Chongqing, China. *Trees*, *33*(3), 719–732. https://doi.org/10.1007/s00468-019-01811-y

Zhao, K., & Popescu, S. (2009). Lidar-based mapping of leaf area index and its use for validating GLOBCARBON satellite LAI product in a temperate forest of the southern USA. *Remote Sensing of Environment*, *113*(8), 1628–1645. https://doi.org/10.1016/j.rse.2009.03.006

SUPPORTING INFORMATION

Additional supporting information can be found online in the Supporting Information section at the end of this article.

How to cite this article: Röll, A., Kang, T., Hahn, P., Ahongshangbam, J., Ellsäßer, F., Hendrayanto, Sharma, P., Wintz, T., & Hölscher, D. (2023). Complex canopy structures control tree transpiration: A study based on 3D modelling in a tropical rainforest. *Hydrological Processes*, *37*(12), e15045. https://doi.org/10.1002/hyp.15045